This is a repository copy of *Self-assembled high molecular weight inulin nanoparticles: Enzymatic synthesis, physicochemical and biological properties*.

White Rose Research Online URL for this paper:
http://eprints.whiterose.ac.uk/144818/

Version: Accepted Version

**Article:**

1    **Self-assembled high molecular weight inulin nanoparticles: Enzymatic**

2        **synthesis, physicochemical and biological properties**

3

4    **Maira Jiménez-Sánchez[1], Rebeca Pérez-Morales[2], Francisco M. Goycoolea[3], Monika**

5    **Mueller[4], Werner Praznik[4], Renate Loeppert [4], Víctor Bermúdez-Morales[5], Guadalupe**

6    **Zavala-Padilla[6], Marcela Ayala[1], Clarita Olvera*[1]**

7

8    *Corresponding author.  Clarita Olvera. E-mail: clarita@ibt.unam.mx

9    1. Departamento de Ingeniería Celular y Biocatálisis, Instituto de Biotecnología, Universidad

10   Nacional Autónoma de México. C. P. 62250, Cuernavaca, Morelos, México. Phone: (52-777)

11   3291619. clarita@ibt.unam.mx, mjims@hotmail.com, maa@ibt.unam.mx

12   2. Laboratorio de Biología Celular y Molecular, Facultad de Ciencias Químicas, Universidad

13   Juárez del Estado de Durango, Campus Gómez Palacio. Tel: +52 (81) 715-8810 ext. 128.

14   rebecapms@ujed.mx

15   3. School of Food Science and Nutrition. University of Leeds. Woodlouse Ln, Leeds LS2 9JT,

16   United Kingdom. F.M.Goycoolea@leeds.ac.uk

17   4. Department of Pharmaceutical Technology and Biopharmaceutics, Vienna University

18   Althanstrasse 14 A-1090 Wien. monika.mueller@univie.ac.at,  werner.praznik@univie.ac.at,

19   renate.loeppert@univie.ac.at.

20   5. Centro de Investigación sobre Enfermedades Infecciosas, Instituto Nacional de Salud Pública,

21   Dirección de Infecciones Crónicas y Cáncer. Avenida Universidad No. 655, Cerrada los Pinos y

22    Caminera, Colonia Santa María Ahuacatitlán, Cuernavaca 62100, Morelos, Mexico;

23    vbermudez@insp.mx

24    6. Unidad de Microscopía Electrónica. Instituto de Biotecnología, Universidad Nacional

25    Autónoma de México. C. P. 62250, Cuernavaca, Morelos, México. Phone: (52-777) 3291861.

26    gzavala@ibt.unam.mx

27

28

29    **Abstract**

30    Inulin has interesting physicochemical and functional properties, and therefore a wide range

31    of applications in the food and medical industries. It has gained great traction due to its

32    ability to form nanoparticles and its possible application as nanovehicle for drug delivery.

33    In this work, we demonstrated that the enzymatically-synthesized high molecular weight

34    (HMW) inulin forms stable spherical nanoparticles with an average diameter of $112 \pm 5$nm.

35    The self-assemblage of HMW inulin nanoparticles is carried out during enzymatic

36    synthesis of the polymer, and become detectable after a certain critical aggregation

37    concentration (CAC) is reached. Both, the CAC and nanoparticle size are influenced by the

38    reaction temperature. These nanoparticles are not toxic for peripheral blood mononuclear

39    cells, at concentrations below 200 μg/mL; no significant prebiotic potential was detected in

40    cultures of 13 probiotic strains. This work contributes to a better understanding of the

41    formation of HMW inulin nanoparticles and their biological properties.

42

43

44  **Highlights**

45  •HMW inulin enzymatically-synthesized is self-assembled into nanoparticles.

46  •The assemblage of inulin nanoparticles is carried out during enzymatic synthesis.

47  •The inulin forms nanoparticles at a critical aggregation concentration (CAC).

48  •The CAC and nanoparticle size are influenced by the reaction temperature.

49  •The inulin nanoparticles are not toxic for peripheral blood mononuclear cells.

50

51

52

53

54

55

56

57

58

59

60  Keywords: Inulin, Polysaccharide nanoparticles, Enzymatic synthesis, Fructan,

61  Inulosucrase.

62

63

64

65

66

67

## 1. Introduction

Fructans are fructose polymers linked by glycosidic bonds which, depending on their origin, have different types of bonds between their monomers, percentage of branching and degree of polymerization (DP) (Madrigal & Sangronis, 2007). Depending on their linkage, fructans are classified as inulin or levan; inulin is a polymer consisting of fructose molecules linked by β (2 → 1) bonds in the main chain and β (2 → 6) bonds within the branches; meanwhile, the levan polymer has β (2 → 6) bonds in the main chain and β (2 → 1) branching (Madrigal & Sangronis, 2007; Stephen, Phillips, & Williams, 2006). In general, fructans produced by plants have a low DP (between 2 and 60 fructose units), while bacterial fructans attain DP > $10^3$ fructose units (Ebisu, Kato, Kotani, & Misaki, 1975; Wada, Sugatani, Terada, Ohguchi, & Miwa, 2005).

Bacterial fructans are synthesized by enzymes known as fructosyltransferases (FTFs). Depending on the polymer, they are classified into: levansucrase (EC 2.4.1.10), the enzyme producing levan, or inulosucrase (EC 2.4.1.9), the enzyme producing inulin (Chambert & Gonzy-Treboul, 1976). The enzymatic synthesis of high molecular weight (HMW) fructans is carried out through sequential transfers of fructosyl residues from sucrose to an acceptor molecule that can be sucrose itself, a growing polymer chain (transferase activity) or a molecule of water (hydrolytic activity) (Chambert & Gonzy-Treboul, 1976). In terms of the polymer molecular weight, reaction conditions are known to affect the size of the synthesized polymer by modulating the enzymatic mechanism (processive or non-processive) (Raga-Carbajal et al., 2016). The DP of these fructans defines its biological and physicochemical properties, which in turn allow a wide spectrum of biotechnological applications.

4

92

93    Fructans can be used for many applications in the food and pharmaceutical industry. Within

94    the food industry, they have been classified as functional ingredients and are generally

95    recognized as safe (GRAS) by the FDA (Handa, Goomer, & Siddhu, 2012). Moreover,

96    fructans are also classified as prebiotic agents, which are defined as non-digestible

97    compounds that may be anaerobically fermented by the beneficial microbiota of the host;

98    these fructans stimulate the bacterial growth that contribute to improve the hosts health

99    (Roberfroid & Slavin, 2000). Furthermore, fructans have been shown to have an

100    immunomodulatory effect on the intestine by increasing the levels of immunoglobulins,

101    interleukins and interferons in peripheral blood mononuclear cells (Watzl, Girrbach, &

102    Roller, 2005). Within the pharmaceutical industry, inulin has been used as tablet coating

103    (Hinrichs, Prinsen, & Frijlink, 2001); it has also been used as vehicle for the administration

104    of drugs through different routes such as oral, respiratory and parenteral routes:

105    subcutaneously, intramuscularly and intravenously (Amorij et al., 2007).

106

107    Recently, research on the ability of fructans to form nanoparticles has fueled research on a

108    new application for using them as nanometric drug carriers. Carboxymethylated low

109    molecular weight inulin has been shown to form nanoparticles for encapsulation of small

110    organic molecules, or as coating agent (Fares & Salem, 2015; Santiago-Rodríguez et al.,

111    2013; Zhang et al., 2014). Moreover, phtalyl inulin nanoparticles have been reported with

112    the capacity to stimulate the production of an antimicrobial peptide by *Pediococcus*

113    *acidilactici* bacteria Kim et al., (2018). There are also recent reports regarding the use of

114    HMW levan in the production of nanoparticles. Sezer, Kazak, Öner & Akbua (2011) used

115    this fructan (> 1,000 kDa) for the nanoencapsulation of albumin as a model protein. The

116  authors demonstrated that the agitation and protein concentration determined the particle

117  size and encapsulation efficiency, obtaining particles within a size of 200-537 nm.

118  Nakapong et al. (2013) reported the isolation of an enzyme from *Bacillus licheniformis* RN-

119  01 able to catalyze the polymerization of fructose; the synthetized fructan was observed to

120  self-assemble into nanoparticles of approximately 50 nm of diameter (Nakapong,

121  Pichyangkura, Ito, Iizuka, & Pongsawasdi, 2013). Furthermore, Kim, Bae & Chung (2015)

122  characterized self-assembled nanoparticles of a HMW levan (>2000 kDa), with an average

123  size of 129.1 $\pm$ 32.8 nm; the nanoparticles could be used to encapsulate indocyanine green

124  for breast cancer diagnosis. Finally, Tabernero A. et al. (2017), obtained nanoparticles of

125  300-500 nm, generated in water by a self-assembling process of a HMW levan produced by

126  *A. nectaris* (Tabernero, González-Garcinuño, Sánchez-Álvarez, Galán, & Martín del Valle,

127  2017). Despite above-mentioned studies demonstrating the fructan self-assembled

128  nanostructuration, no report exists regarding a deep analysis of the HMW fructan

129  nanoparticles production during the enzymatic synthesis of the polymer. Besides, no studies

130  about HMW inulin nanoparticles production and characterization have been reported.

131  In this work, we performed an analysis of the production of self-assembling inulin

132  nanoparticles during the enzymatic synthesis of HMW polymer and the effect of reaction

133  conditions over the synthesis and the size of fructan nanoparticles using the inulosucrase

134  from *Leuconostoc citreum*. In addition, we analyzed the physicochemical and biological

135  characteristics of these nanoparticles with the future objective of developing a nano-

136  controlled release system for small molecules and biomolecules.

137

138

**2. Materials and methods**

*2.1 Materials*

Isopropyl β-D-1-thyogalacto-pyranoside and kanamycin were purchased from Gold Biotechnology, Inc., St Louis, MO, USA. Complete EDTA-free was from Roche (Mannheim, Germany) and Bradford reagent was from Bio-Rad (Hercules, CA). Bovine serum albumin (BSA albumin fraction V) was provided by Sigma Aldrich (St. Louis, MO, USA). Lymphoprep and RPMI medium were purchased from Invitrogen, Thermo Scientific (Austin, TX, USA), while L-glutamine was form Gibco Thermo Scientific (Austin, TX, USA). All other agents used were of analytical grade.

*2.2 Preparation of Escherichia coli cell extracts and purification of IslA4*

*Escherichia coli* BL21 cells transformed with the pET28a-*IslA4* gene were grown in Luria Bertani broth containing 50 μg/mL$^{-1}$ kanamycin at 37 °C and 120 rpm. The culture was induced with 0.2 mM isopropyl β-D-1-thyogalacto-pyranoside. Once the cells reached an optical density of 0.6 (OD$_{600}$, λ=600 nm) they were incubated at 18 °C for 6 additional hours. The cells were then harvested by centrifugation (2,500 × g for 10 min) and the resulting pellet washed twice with a 50 mM phosphate buffer (pH 6.0) containing 1 mM CaCl$_2$ before being re-suspended in 5 mL of the same buffer containing Complete EDTA free (one tablet to 50 mL of cell extract), which were added as protease inhibitors, and sonicated. Cell debris was removed by centrifugation (21,130 × g for 30 min) and the supernatant containing the enzyme was recovered for further processing. The protein concentration was determined according to the Bradford method (Bradford, 1976) using bovine serum albumin (BSA) as standard. The enzyme was purified by Fast Protein Liquid

163 Chromatography (FPLC) on an ÄKTA prime (Amersham Biosciences, Uppsala, Sweden)

164 using a cation exchange CM-Sepharose column (GE Healthcare, Uppsala Sweden). The

165 elution was performed with a phosphate buffer at pH 6.0 (gradient of 0.1 to 1.0 M). The

166 eluted fractions were transferred to molecular filters to concentrate (Millipore molecular cut

167 10,000 Da) and centrifuged for 20 min at 3,700 x g before addition of 100 mM acetate

168 buffer pH 6 (supplemented with 1 mM $CaCl_2$) to the molecular filters. The purity of IslA4

169 was verified by SDS-PAGE.

170

171 *2.3 Activity assay*

172 Initial reaction rates were measured at 30 °C in 100 mM phosphate buffer (pH 6.0)

173 containing 1 mM $CaCl_2$ in the presence of 292 mM sucrose. The global activity was

174 expressed as the reducing sugars released from sucrose using the 3,5-dinitrosalicylic acid

175 method (DNS) (Miller, 1959). One *global* activity unit (U) was defined as the amount of

176 enzyme required to produce 1 μmol of reducing sugars per minute. The specific hydrolysis

177 and transferase activities were measured by HPLC based on the amounts of fructose and

178 glucose. The HPLC method used in the current study is described below.

179

180 *2.4 Carbohydrate analysis*

181 Carbohydrates were quantified by high-pressure liquid chromatography (HPLC) using a

182 Waters 600E system controller (Waters Corp. Milford, MA, USA) equipped with a

183 refractive index detector (Waters 410) using a Prevail Carbohydrate ES column

184 $(250 \times 4.6 \text{ mm})$ at 30°C. The HPLC system was run with a mobile phase consisting of a

185 75:25 (v/v) mixture of acetonitrile and water at a flow rate of 1.0 mL/min$^{-1}$. The molecular

186 weight of inulin was determined by Size Exclusion Chromatography (SEC) using a serial

187    set of Ultrahydrogel (UG 500 and linear) columns at 30°C with a refractive index detector

188    (Waters 410). The columns were run with a mobile phase sodium nitrate 100 mM at a flow

189    rate of 0.8 mL/min. Oligosaccharides were separated and analyzed by high-performance

190    anion exchange chromatography with pulsed amperometric detection (HPAEC-PAD,

191    Dionex), using a CarboPac PAD-200 column (250 × 2 mm, Dionex). The following

192    gradient was used: eluent A at 100% (0 min), 99% (0.5 min), 80% (25 min), 20% (85 min)

193    and 100% (95 min). Eluent A was 150 mM sodium hydroxide and eluent B was 150 mM

194    sodium hydroxide in 500 mM sodium acetate.

195

196    *2.5 Reductive methylation analysis (reductive cleavage method)*

197    Methylation, reductive cleavage, and acetylation were performed according to established

198    procedures (Praznik, Löppert & Helmut, 2007; Rolf & Gray, 1984). Well defined [(2-1)-

199    linked β-D-Fruf] linkage-types of inulin from chicory (Orafti, Co; house prepared samples)

200    and of house-prepared [(2-6)-linked b-D-Fruf] fructan from *Pucinellia peisonis* were

201    applied as standards. Gas cromatography identification was performed on Shimadzu GC

202    2010 with a capillary column (DB 1701; 30 m, 0.25 mm i.d.: 0.25l m film thickness;

203    Agilent, Co.), helium as carrier gas and FID (flame ionization detection) with the following

204    temperature program: 80 →135 °C at 10 °C/min, 135 → 155 °C at 2°C/min, 155→200 °C

205    at 3 °C/min, 200→260 °C at 5 °C/min. The injector and detector temperatures were 230°C

206    and 270°C respectively. Measurements were performed with a split ratio of 1:5 in triplicate.

207    The relative amount of each residue and the ratio of β-D-fructose- and α-D-glucose-

208    residues in the molecules were computed as the molar percentages from response-factor

209    corrected GC/FID peak areas; the ratio of β-D-fructose and α-D-glucose-residues assumes

210    one α-D-glucose residue for each molecule (Praznik, Löppert, & Helmut, 2007).

211

212    *2.6 Study of nanoparticles formation during enzymatic inulin production*

213    A more stable, truncated version (IslA4) of the IslA enzyme produced by *L. citreum* CW28

214    was used as catalyst to study the formation of nanoparticles during the polymer synthesis.

215    IslA4 lacks the N- and C-terminal regions, does not present auto-proteolysis and retain the

216    ability to produce inulin of the same molecular weight as the wild-type enzyme (Del Moral,

217    Olvera, Rodriguez, & Munguia, 2008). The enzymatic reactions were carried out using 0.5

218    U/mL of IslA4 enzyme and a sucrose concentration of 100 g/L in a 0.1 M sodium acetate

219    buffer, pH 6.0 supplemented with 1 mM $CaCl_2$ and a temperature of 30°C under constant

220    stirring. The reaction was stopped by boiling the samples for 5 min to inactivate the

221    enzyme. All the reactions were allowed to proceed until they reached a sucrose conversion

222    of approximately 90%. The reaction specificity (i.e., hydrolysis to transferase ratio) was

223    determined by measuring the amounts of glucose and fructose released during the reaction.

224    Free glucose (Gf) was derived from hydrolyzed sucrose as well as the sucrose was used as a

225    fructose donor for the transferring reactions, whereas free fructose (Ff) was derived

226    exclusively from the hydrolytic activity of the enzyme. The difference between the amounts

227    of consumed and hydrolyzed sucrose could therefore be used to determine the amount of

228    fructose used for transfructosylation (Ft) (*i.e.*, transferase activity).

229

230    *2.7 Test of the effect of the reaction conditions on the inulin nanoparticle size*

231  For each reaction a sucrose concentration of 100 g/L and 0.5 U/ml of inulosucrase IslA4

232  was used in sodium acetate buffer (pH 6.0) supplemented with 1 mM $CaCl_2$ with varying

233  the concentration of 50, 100 and 200 mM (ionic strength $\mu$ of 0.005, 0.1 and 0.2

234  respectively) at a temperature of 30, 18 and 4 °C under constant stirring. The nanoparticle

235  size was measured after 24 hours of starting the enzymatic reaction.

236

237  *2.8 Determination of the size distribution of nanoparticles*

238  The intensity size (hydrodynamic diameter) distributions of the inulin nanoparticles were

239  determined by dynamic light scattering (DLS) with non-invasive back scattering on a

240  Zetasizer NanoZS instrument (Malvern Instruments Ltd., Malvern,UK) equipped with a 4

241  mW helium/neon red laser ($\lambda$ = 633 nm) and the detection was at an angle of 173 °.

242  Measurements were performed at 30, 18 and 4 °C using 50 $\mu$l from the enzymatic reaction.

243  Analyses were performed in three different batches and the results were expressed as a

244  mean of three measurements. The Zeta-potential was measured by phase analysis light

245  scattering and mixed laser Doppler velocimetry (M3-PALS) in the same instrument.

246  Measurements were performed at 30ºC by diluting an aliquot of 50 $\mu$L from the enzymatic

247  reaction in water.

248

249  *2.9 Nanoparticle tracking analysis (NTA)*

250  NTA measurements were performed using a NanoSight LM10 instrument (NanoSight,

251  Amesbury, UK), consisting of a conventional optical microscope, Marlin charged coupled

252  device (CCD) camera, and a LM10 unit (sample unit) with a laser light source. LM10 is the

253 first generation instrument from the NanoSight Company, which in the mean time has

254 developed devices with additional features and upgraded software.

255 Following the manufacturer's instructions, we serially diluted all samples with sterile water

256 or DPBS to reach a particle concentration suitable for the analysis with NTA ($1.0 \times 10^8$ to

257 $2.5 \times 10^9$ particles/mL). We prepared at least two different sample dilutions for each sample

258 and analyzed each one twice. The samples were injected into the LM unit (approximately

259 300 µL) with a 1 mL sterile syringe. The capturing settings (shutter and gain) and analyzing

260 settings were manually set according to the protocol suggested in the Technical note "How

261 to make Concentration Measurements using NanoSight Equipment" (Technical Note,

262 NanoSight, last updated 17/06/09) and then optimized for a specific virus or the latex

263 particles. The NanoSight LM10 recorded 60-second sample videos that were then analyzed

264 with the Nanoparticle Tracking Analysis (NTA) 2.0 Analytical software release version

265 build 0125.

266

267 *2.10 Transmission electron microscopy (TEM) analysis inulin NPs*

268 Five µL were taken from the enzymatic reaction and dropped onto a carbon–copper grid

269 and air dried for 24 h. The excess sample was then removed with a filter paper and allowed

270 to float on a drop (5 µL) of 2 % uranyl acetate for 1 min. The excess of uranyl is also

271 removed with the aid of a filter paper. The grids with the samples tested by the negative

272 staining method were observed in a transmission electron microscope brand ZEISS model

273 Libra at an acceleration voltage 120 Kv with Gatan digital camera.

274

275 *2.11 Cytotoxicity tests*

276    The cytotoxicity assay was performed with neutral red assay based on an already published

277    protocol (Repetto, del Peso, & Zurita, 2008). This method determines the accumulation of

278    the neutral red dye in the lysosomes of viable cells. Three experiments were performed in

279    triplicate. Peripheral blood mononuclear cells (PBMC's) were obtained from a pool of 3

280    samples from clinically healthy women, ranging in age from 28-37 years. Cells were

281    purified by density gradient with Lymphoprep. 50,000 cells were cultivated in RPMI

282    medium supplemented with 5 % of fetal bovine serum and 1 % of L-glutamine. Exposure

283    treatments with inulin polymer were at concentrations of 25, 50, 100, 150 and 200 μg/mL

284    by 24 h, followed by an incubation for 2 h with neutral red dye (4μg/mL) dissolved in

285    serum free medium. Cells were washed with 1X phosphate buffer, 1 mL of of elution

286    solution (EtOH/AcCOOH, 50/1 % v/v) was added, followed by gentle shaking. Aliquots of

287    the resulting solutions were transferred to 96-well plates and absorbance at 540 nm was

288    recorded using the microplate spectrophotometer system (Spectra max190-Molecular

289    Devices).

290    The percentage of viability was obtained using the following formula:

291                            %Viability = OD treated cells x100 / OD control cells*

292    A one-way ANOVA test was performed for multiple comparisons with Dunnet's ad hoc test

293    comparing treatments against the untreated control group using GraphPad Prism 7.01

294    software. A 24-hour treatment with ethanol was used as a positive cell death control*.

295

296    *2.12 Determination of the prebiotic potential*

297    Growth curves of the probiotic strains in the presence of *Leuconstoc citreum* inulin were

298    determined by turbidity measurement using Bioscreen C (Oy Growth Curves Ab Ltd,

299    Helsinki, Finland). With this method, the change of the $OD_{600}$ value was measured

300    indicating bacterial growth. A fresh overnight culture was prepared. The cell amount

301    required for a starting $OD_{600}$ of 0.1 was harvested, washed three times in phosphate

302    buffered saline (PBS) supplemented with 0.5 g/L cysteine hydrochloride, and resuspended

303    in MRS-medium without sugar. The negative control was incubated without sugar, whereas

304    the samples were incubated in the presence of 1% sugars, in honeycomb plates at 37 °C for

305    48 h and the $OD_{600}$ was measured every hour after mixing for 15 s. The growth curves were

306    determined 3 times and the results are shown as a mean.

307

308    **3. Results and Discussion**

309

310    **3.1 Nanoparticles presence and physicochemical properties of HMW inulin from**

311    ***Leuconostoc citreum***

312    Considering the self-assembly in water of HMW levan nanoparticles which is already

313    reported (Kim, Bae & Chung, 2015; Nakapong et al., 2013; Tabernero et al., 2017), we

314    decided to assess nanoparticles presence in enzymatically-synthesized HMW inulin, using

315    complete cells of *Leuconostoc citreum* as described by Ortiz-Soto, Olivares-Illana, &

316    López-Munguía, (2004). The results obtained by dynamic light scattering (DLS) showed

317    the presence of nanoparticles with a size distribution between 50 nm and 300 nm, a Z-

318    average of the calculated diameter of 112 ± 5 nm and a polydispersity index (PI) of 0.069 ±

319    0.01 (Table 1). These results confirm the presence of HMW inulin nanoparticles with

320    similar values to those reported for self-assembled HMW levan nanoparticles, were the Z-

321    average was 129 ± 32 nm (Nakapong et al., 2013); the molecular weight of the levan used

322    in that study was >2000 kDa, similar to the HMW inulin used in the present work (Table

323    1). Nakapong et al., (2013), reported self-assembled nanoparticles with 50 nm diameter,

324  using a 612 kDa molecular weight levan. On the other hand, Tabernero et al., (2017),

325  obtained self-assembled nanoparticles from a HMW levan (6,000 kDa) with a size ranging

326  from ~300 to ~500 nm. It is possible that in the case of HMW fructans, a low molecular

327  weight lead to smaller nanoparticles, compared to high molecular weight generating larger

328  nanoparticles. This could be also a consequence of the branching and larger hydrodynamic

329  diameter of HMW polymers (Wolff et al., 2000).

330

331  Table 1. Physicochemical characteristics of HMW inulin produced by *Leuconostoc citreum*.

| Characteristic | Value | Source |
|---|---|---|
| Molecular weight | 90 a 4,400 kDa | (Olivares-Illana, et al., 2002; Del Moral et al., 2008) |
| Molecular weight average | 3,000 kDa | (Del Moral et al., 2008) |
| Degree of polymerization | 18, 500 | (Del Moral et al., 2008) |
| Hydrodynamic diameter | $112 \pm 5nm$ | Present work |
| Polydispersity index diameter | $0.069 \pm 0.01$ | Present work |
| Branching percentage | $10.03 \pm 1 \%$ | Present work |
| Number of nanoparticles per ml | $2.83 \pm 0.2 \times 10^{12}$ | Present work |
| Z Potential | $-10 \pm 1.8$ mV | Present work |

332

333  Table 1, summarizes the physicochemical properties of HMW inulin obtained using the

334  inulosucrase from *L. citreum* CW28, as previously reported and as obtained in this work.
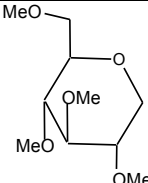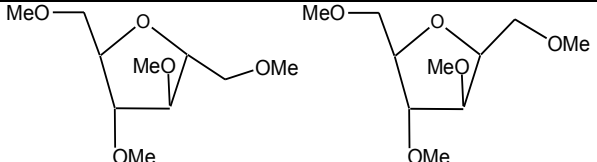
335

336  Polymer identification by NMR was previously reported by Olivares-Illana et al., 2002 and

337  re-analyzed together with other properties in our workgroup (molecular weight, molecular

338  weight average, and degree of polymerization) (Del Moral et al., 2008). In order to deepen

339  the molecular characterization of this polymer, physicochemical properties were
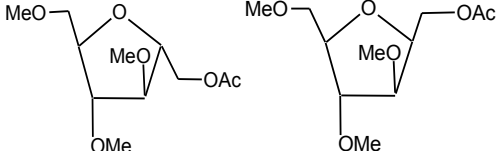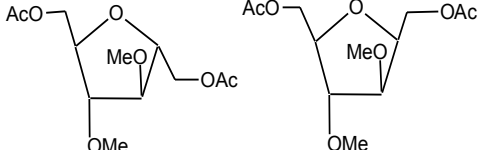
340  determined. For instance, the branching percentage was determined by reductive

341  methylation analysis and GC/FID identification. Considering a molecular weight of 3,000

342  kDa, it was determined that the HMW inulin from *L. citreum* contains approximately

343  ~18,519 fructose molecules, of which ~14,730 are linear fructose molecules, ~858

344  branched fructose, and ~1,899 terminal fructose molecules. According to the relative

345  amount of terminal fructosyl residues, the inulin of *Leuconostoc citreum* has a branching

346  percentage of 10.03%, suggesting that there is a branch every 8 fructose units (Table 2).

347  This branching percentage is greater than those reported for other HMW inulins; for

348  example, 20,000 kDa inulin synthesized by a fructosyltransferase of *Streptococcus mutans*

349  presents a branching percentage of 6.1%, whereas a mixture of low and high molecular

350  weight inulin (14.9-5,000 kDa) produced by *Aspergillus sydowi* IAM 2544 has a branching

351  percentage of 5.4 % (Wolff et al., 2000). This higher branching percentage could influence

352  the size and packing density of the nanoparticles, as Wolff et al., (2000) has been shown

353  before for those inulin nanoparticles.

354

355  Table 2. Percentage (%) and number (n) per molecule of β-D-Fruf and α-D-Glcp residues

356  obtained by reductive methylation analysis, from HMW inulin produced by *Leuconostoc*

357  *citreum.*

| Fraction | % | Chemical structure |
|---|---|---|
| Terminal Glucose | 0.17 |  |
| Terminal Fructose α and ß | 10.25 |  |

| | | |
|---|---|---|
| **Fru-lineal-2,1 α and ß** | 79.54 |  |
| **Branched-Fructose α and ß** | 10.03 |  |

358

359 Besides branching, other physicochemical characteristic that could influence the glomerular

360 structure of polymers is the Zeta-potential (Wolff et al., 2000). The Zeta-potential is a value

361 that represents the electrostatic behavior of colloidal particles in the medium; it is related to

362 the aggregation tendency of the particles in solution, so it is considered to reflect the

363 stability of the colloidal system (Sundar, Kundu, & Kundu, 2010). The Zeta-potential value

364 determination yielded a value of -10 ±1.8 mV, indicating a slight negative charge. This

365 value is similar to that for inulin nanoparticles that we have reported in a previous study

366 (Sarkar et al., 2018) and is not far from that found by Carneiro-Da-Cunha, Cerqueira,

367 Souza, Teixeira, & Vicente, (2011) for galactomannan polymer in solution. This last

368 polymer is neutral like inulin, whose skeleton is formed by β-D-mannopyranose units

369 linked by bonds (1→4), also containing α-D-galactopyranose branches joined by bonds

370 (1→6). The Zeta-potential values obtained for galactomannan nanoparticles, produced by

371 *Caesalpinia pulcherrima* and *Gleditsia triacanthos*, were -5.7 and -4.98 mV respectively

372 (Carneiro-Da-Cunha et al., 2011).

373 There are previous reports of formation of chemically modified low molecular weight

374 inulin nanoparticles, such as inulin-carboxymethylated used to encapsulate magnetic

375 nanoparticles (iron oxide) and phtalyl inulin nanoparticles (Kim, Bae & Chung, 2015; Kim

376 et al., 2018). Also, it has been documented the production of nanoparticles modified with

377    ibuprofen and the conjugated inulin with curcumin to form nanoparticles and thus achieve

378    the solubility required for the release of this polyphenol (Fares & Salem, 2015; Santiago-

379    Rodríguez et al., 2013; Zhang et al., 2014). However, in such studies, the Zeta-potential

380    was not measured directly and was only deduced from electrophoretic mobility of charged

381    particles under an applied electric field (Bhattacharjee, 2016). Accordingly, if the

382    nanoparticle is chemically modified with another molecule, it will affect the final Zeta-

383    potential value. Considering that inulin is a neutral polymer, it was not expected to obtain a

384    Zeta-potential value that reveals the existence of some residual surface charge. Thus it was

385    suggested that this value could be attributed to the presence of some negatively charged

386    component attached to the surface of these nanoparticles. The amount of protein present in

387    the sample was $9.52 \times 10^{-3} \pm 0.28$ mg/ml, despite being a relatively low amount of protein, it

388    could be responsible for the slight negative charge yielded. In general, particles whose

389    Zeta-potential is within the range of +30mV and -30mV are considered to have a tendency

390    to aggregate (Wongsagonsup, Shobsngob, Oonkhanond, & Varavinit, 2005). Given that,

391    the Zeta-potential of inulin nanoparticles is within this range, the particles may be unstable.

392    In order to confirm this, changes in size were monitored for 15 days by DLS. The

393    hydrodynamic diameter was constant, suggesting that despite the low Zeta-potential value,

394    the nanoparticles are stable and do not tend to aggregate.

395

396    The quantification of the number of nanoparticles in solution was $2.83 \times 10^{12}$

397    nanoparticles/mL (Table 1), these particles were individually visualized and a size

398    distribution of ~32 to ~232 nm was observed upon analysis of a sample containing 5 g/L of

399    HMW inulin. Within this distribution, the particle size mode was 84.4 ± 24.5 nm, with a

400    concentration of $42.61 \times 10^{10}$ nanoparticles/mL.

401

**3.2 Study of inulin nanoparticles formation during enzymatic synthesis.**

In order to elucidate whether the inulin nanoparticles are formed during the enzymatic

synthesis, a truncated version of the IslA enzyme produced by *L. citreum* CW28, IslA4,

was used. IslA4 lacks the N- and C-terminal regions does not present auto-proteolysis, and

retains the ability to produce inulin of the same molecular weight as the wild-type enzyme

(Del Moral, Olvera, Rodriguez & Munguia, 2008). Both, polymer production and particle

size were monitored during the enzymatic reaction by DLS analyses. The reaction was

followed for 36 h, reaching a final nanoparticle size of 97 nm and a final inulin

concentration of 22.91 g/L, as shown in Figure 1A. The appearance of nanoparticles was

detected after 30 min of reaction when produced inulin was 15.17 g/L. The average

hydrodynamic diameter of these nanoparticles was 67.33 nm (Figure 1B). The sudden

appearance of inulin nanoparticles during the polymer synthesis suggests that there might

be an inulin critical aggregation concentration (CAC). It is proposed that the CAC is the

amount of polymer required for the assembly of nanoparticles (Dan, Ghosh, & Moulik,

2009). In the case of HMW inulin we determined a CAC of 15.17 g/L for the assembly of

the nanoparticles under the studied conditions (Figure 1A). The identification of CAC has

already been reported for the self-assembly of low molecular weight inulin nanoparticles

where, the aggregation concentration was 0.072 g/L, generating nanoparticles of 180 nm

(Dan et al., 2009). This concentration is two orders of magnitude lower than the observed in

the present work; this discrepancy is probably due to the difference in size and branching

between the polymers.

423
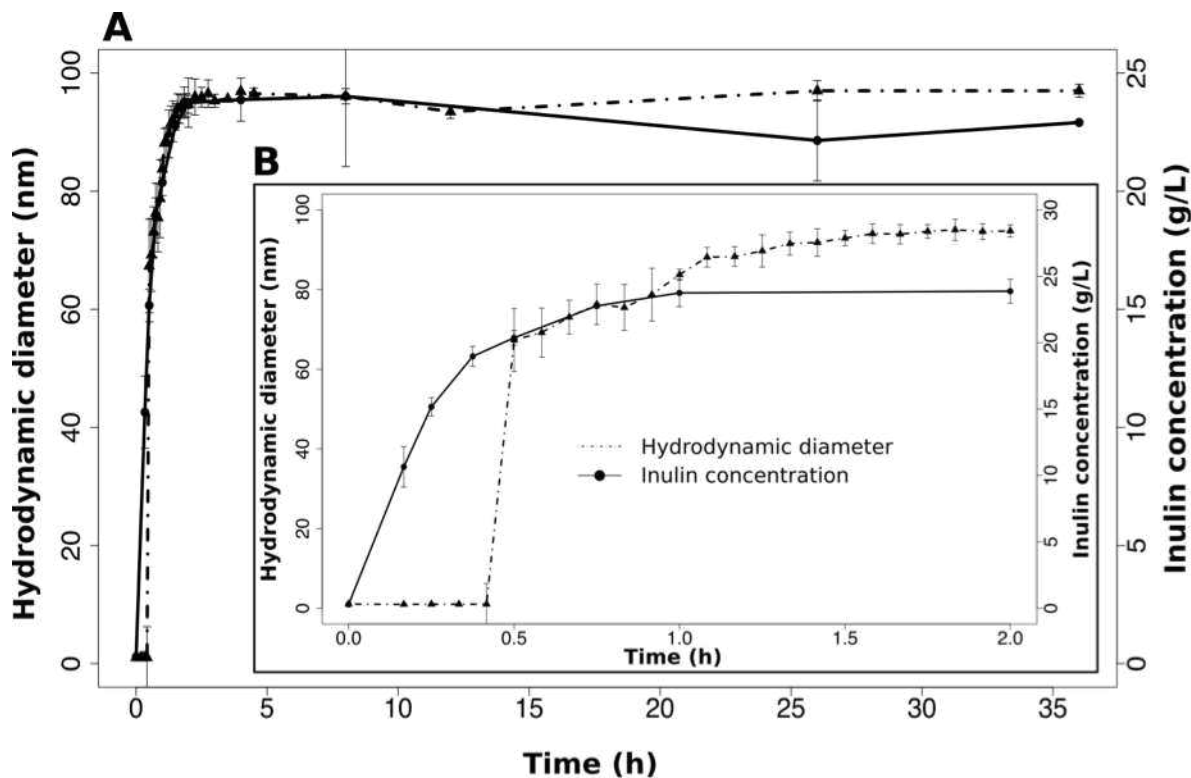
Figure 1. Kinetics of inulin production (solid line) and evolution of the hydrodynamic diameter average of inulin nanoparticles (dot-dashed line). Reaction conditions 0.5 U/ml of IslA4, 100 g/L sucrose at 30°C in 100 mM buffer pH 6. Insert: first 2 h of the reaction.

427

In order to determine the morphology of the observed nanoparticles, transmission electron microscopy (TEM) was performed. Figure 2, shows micrographs of the reaction mixture after 36 h, corresponding to 95% sucrose conversion and 22.9 g/L inulin. In these micrographs, spherical particles of various sizes can be observed which are within the size distribution determined by DLS (Figures 2A and B). Figure 2C shows two isolated nanoparticles of ~260 and ~280 nm approximately where, in addition to the circular morphology, a concave structure is observed, thus suggesting that these nanoparticles could be hollow. However, further analysis by scanning electron microscopy (SEM) imaging and spectroscopic ellipsometry could corroborate the validity of this hypothesis. Based on these

20

437 results, we can conclude that HMW inulin arranges into self-assembled nanoparticles

438 during the enzymatic synthesis of the polymer, catalyzed by IslA4.

439
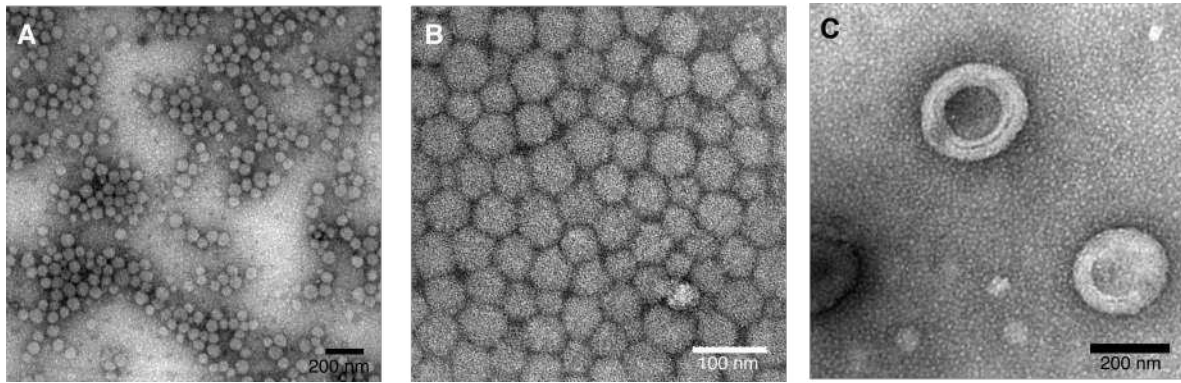
440 

441

442 Figure 2. TEM micrographs of inulin nanoparticles produced during an enzymatic reaction

443 using IslA 4 (0.5 U/ml, 100 g/L sucrose) after a 36 h-reaction. A) 10k B) 20k C) 40k

444

445 **3.3 Effect of reaction conditions on the inulin nanoparticles formation**

446 The influence of physicochemical factors such as temperature and ionic strength on the

447 formation of polysaccharide nanoparticles has already been reported (Carneiro-Da-Cunha

448 et al., 2011; Kumar et al., 2015; Li, Jiang, Chen, Yang, & Guan, 2004; Nakapong et al.,

449 2013; Sharma, Madan, & Lin, 2016). Cations can affect the conformational properties of

450 the nanoparticles since they might interfere with the hydrogen bonds within the structure

451 (Li et al., 2004). On the other hand, the temperature can affect not only the rheological

452 behavior of inulin, but also the enzymatic reaction rate that in turn could influence the

453 nanoparticle formation (Kumar et al., 2015). In order to analyze the effect of the ionic

454 strength and temperature on the hydrodynamic diameter of the enzymatically synthesized

455 inulin nanoparticles, we performed the enzymatic reaction using different buffer solution

456   concentrations and three temperatures 4, 18 and 30°C. The hydrodynamic diameter average

457   of the inulin nanoparticles was determined by DLS at 90% sucrose conversion. As depicted

458   in Figure 3, minimal variation of the particle size was observed when the ionic strength was

459   modified. This was confirmed when a correlation study between these variables was

460   performed using the R Studio program. The value obtained for the correlation between the

461   ionic strength and the particle size was 0.17, demonstrating that there is no significant

462   correlation for this range of salt concentration.

463
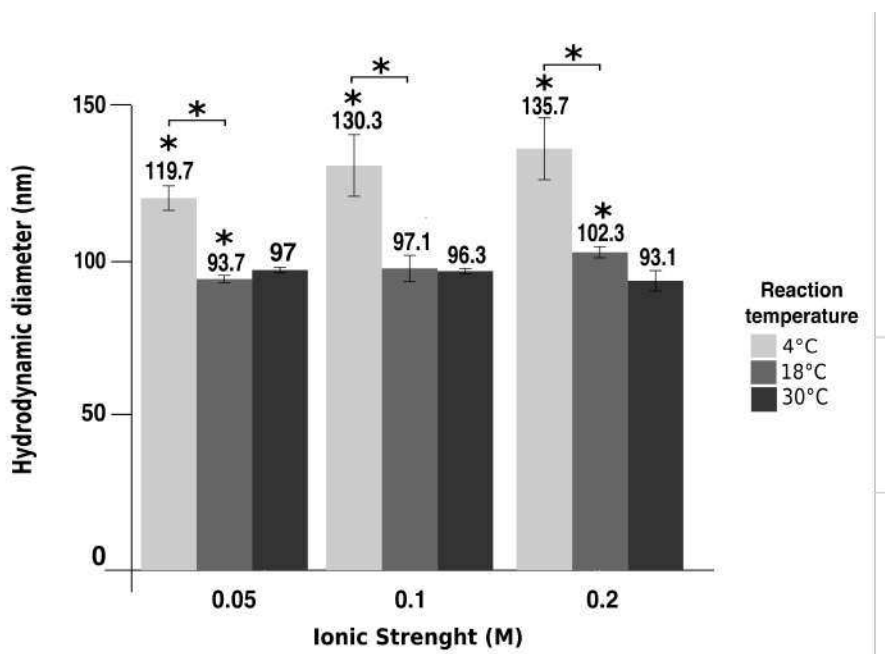


464

465   Figure 3. Average hydrodynamic diameter in function of ionic strength and temperature.

466   Measurements were performed by DLS using 50μl of reactions Reaction conditions: 0.5

467   U/ml of IslA4, 100 g/L sucrose, buffer pH 6 at 24 hours after starting the enzymatic

468   reaction.

469   On the other hand, it was observed that decreasing the temperature resulted in a

470   nanoparticle size increase. The highest effect was observed between a 30 and 4°C reaction

471     in a 0.2 M buffer, obtaining a 32% increase in nanoparticle size. Regarding the correlation

472     between temperature and particle size, a high negative correlation was observed (-0.88),

473     which shows that the temperature is a factor with a strong influence on the formation of the

474     nanoparticles. Considering these results, our focus was only on the temperature effect on

475     the nanoparticle size. It has been suggested that temperature can affect nucleation and

476     particle growth (Thanh, Maclean, & Mahiddine, 2014). This growth is usually slower at a

477     lower temperature, favoring the kinetic stabilization process of the nanoparticles, which

478     will promote larger and more stable particles. Also, by reducing the temperature the

479     reaction rate for the enzyme IslA4 decreases and so does the production rate of the polymer

480     (Del Moral et al., 2008).

481

482     To examine the effect of the temperature at 4ºC on the evolution of the nanoparticles

483     hydrodynamic diameter, we monitored an enzymatic reaction for 36 h under the same

484     conditions described above but at greater temperature. As seen in Figure 4A, the sudden

485     appearance of the nanoparticles also occurs under these conditions; however, the time of

486     appearance and inulin concentration were different from those at 30 ºC. The nanoparticles

487     appear at an inulin concentration of 6.78 g/L, 1.5 h after the reaction started and at substrate

488     conversion of 32 % (Figure 4B). The critical aggregation concentration was 44 % lower

489     than that recorded at 30 °C, and consequently, also a lower substrate conversion (32 vs 58

490     %) was required to observe the nanoparticles. This is the first study where the nanoparticle

491     size and formations are monitored during an enzymatic reaction.

492
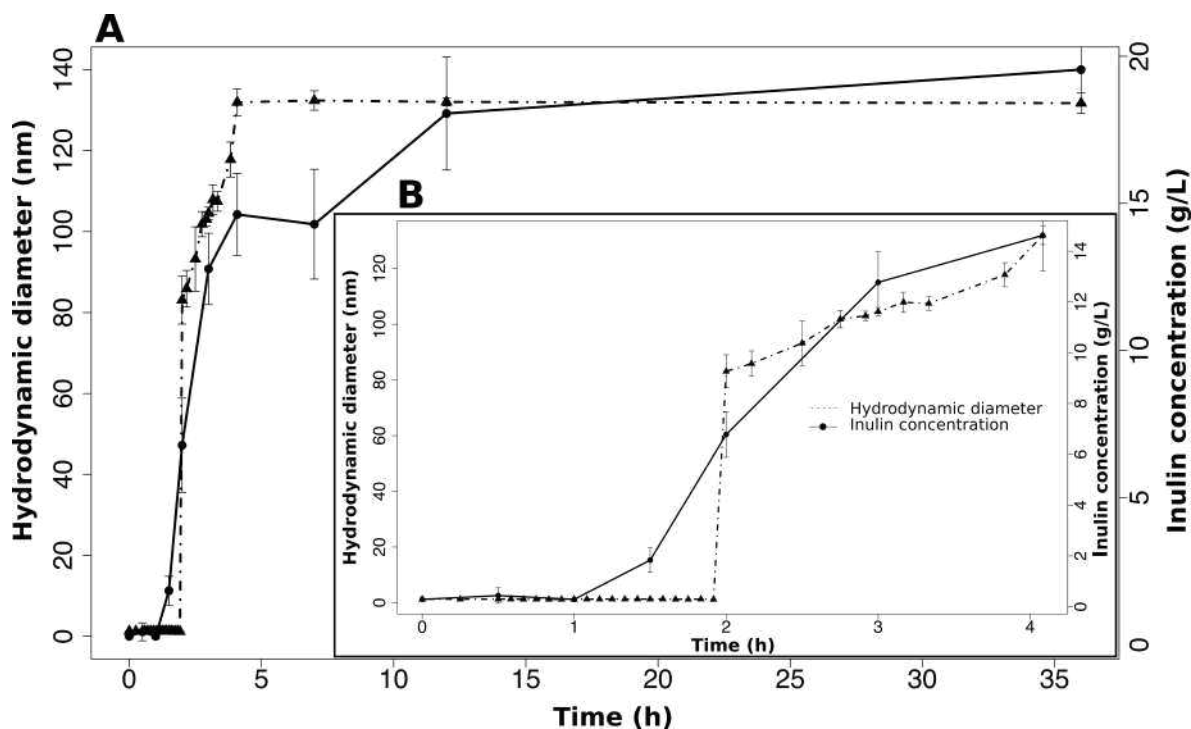
493
494

495    Figure 4. Kinetics of inulin production (solid line) and evolution of the hydrodynamic

496    diameter average of inulin particles (dot-dashed line). Reaction conditions: 0.5 U/ml of

497    IslA4, 100 g/L sucrose at 4°C in 100 mM buffer pH 6. Insert: first 4 h of the reaction.

498

499    Regarding the effect of temperature on the onset of nanoparticle formation, a lower

500    temperature could favor the nucleation rate thus requiring a lower inulin concentration to

501    observe the particles. Other factors that could influence the process, such as the molecular

502    weight of the fructans, are not a determinant in this case.  For instance, an increase in the

503    molecular weight of the levan synthesized by the *B*. *subtilis* levansucrase (SacB) has been

504    reported as the reaction temperature decreased to 4 °C (Porras-Domínguez, Ávila-

505    Fernández, Miranda-Molina, Rodríguez-Alegría, & Munguía, 2015). However, for IslA4

506     the molecular weight of the polymer remains the same whether the reaction takes place at

507     30 or 4 °C (data not shown).

508

509     The morphology of inulin nanoparticles enzymatically synthesized at 4 °C was analyzed by

510     TEM. In Figure 5, spherical nanoparticles of 80 to 130 nm are observed (Figure 5A) which

511     are consistent with data recorded by DLS (Figure 4) and morphologically similar to those

512     observed in reactions at 30°C (Figure 2). However, large amorphous aggregates can also be

513     observed as well as fibers with a thickness of about 20 nm (Figure 5B). These results are

514     similar to those already reported in 2015, were they observed nanoparticles and fibers of

515     chicory inulin by TEM (Cooper et al., 2015).

516
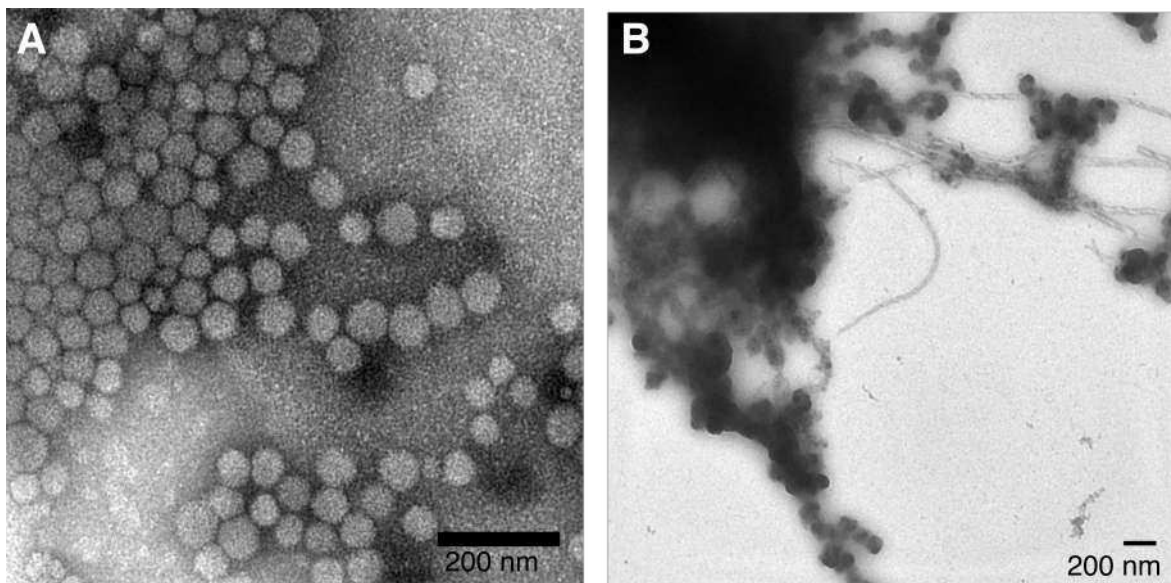


517

518     Figure 5. TEM micrographs of inulin nanoparticles, enzymatically synthesized, at 4°C and

519     after 73% substrate conversion. A) 20 K, B) 6.3 K.

520     The presence of these amorphous aggregates together with the increase in the average of

521     the hydrodynamic diameter of the inulin nanoparticles enzymatically synthesized at 4 °C,

522   reinforces the notion that the reaction conditions mainly affect the structuring of the

523   nanoparticles. The temperature could be directly affecting the molecules of inulin by

524   reducing their movement, allowing these molecules to arrange in such way that they form

525   fibers, possibly as intermediates, favoring the existence of larger and stable spherulite-type

526   particles. This type of morphology consists of several lamellae branching from a central

527   nucleus, and it could be possible that lamellae are structured by the observed fibers (Cruz

528   Herrera, 2012).

529

530   **3.4 Nanoparticles biological properties**

531   *3.4.1 Cytotoxicity*

532   Natural polysaccharides are effective nanocarriers for delivery of active ingredients or

533   drugs. In this study, no cytotoxicity was observed at concentrations of 50-200 μg/ml,

534   concerning to negative control (without inulin nanoparticles) and cell viability remained

535   above 85% in all treatments, while the positive control significantly decreased the viability

536   percentage as shown in Figure 6. The concentrations analyzed did not generate cytotoxicity,

537   in addition, polysaccharides such as inulin can stimulate the immune response through the

538   activation of interleukins and interferon (Vogt et al., 2014). In another study, it was

539   observed that fructan polymers could protect intestinal epithelial cells against harmful

540   agents, so their properties like probiotic are preserved Vogt et al., 2013.

541   Ahmed, Zahran & Emam (2016) analyzed different formulations of nanoparticles based on

542   polysaccharides and no cytotoxicity was observed. Thus, it is suggested that they are safe in

543   their administration as a vehicle, due to their versatility and low toxicity have been used as

544   a vehicle for the release of chemotherapeutic agents (Ahmed, Zahran, & Emam, 2016).

545

546
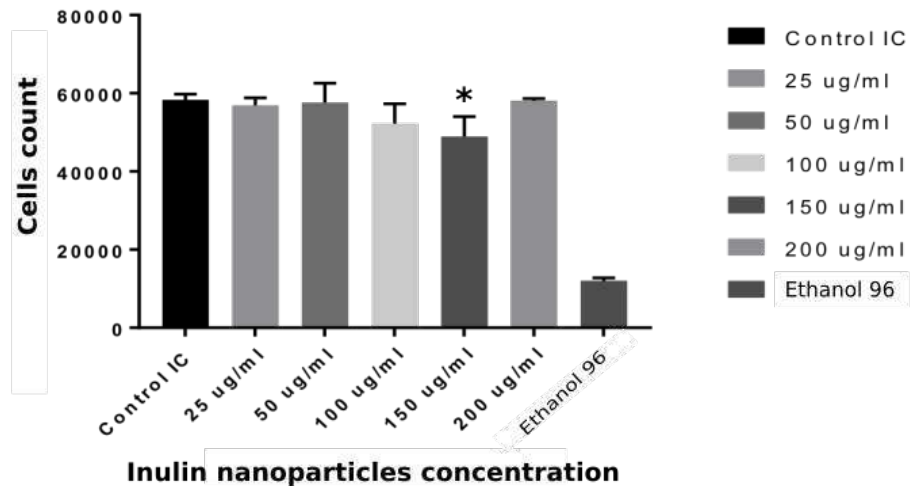
Figure 6. The concentration range was 50 – 200 µg/mL. Viability was decreased in the concentration of 50 µg/mL (p = 0.04) and 150 µg/mL (p = 0.02) these differences were significant with respect to the control. Although these data are significant, cell viability remains above 85%. One-way ANOVA test followed by Dunnet's multiple comparison test was applied to compare treatment with controls. Three independent experiments in triplicate were performed and results are expressed as means ± SDs.  * P values < 0.05 were considered statistically significant.

*3.4.2 Prebiotic potential*

Considering the null toxicity of inulin and their ability to reach the intestine virtually intact, due to their resistance to direct degradation by the host, these HMW inulin nanoparticles could be ideal as colon site-directed drug carriers, where they could be degraded by the microbiota. However, there are no reports on the prebiotic potential of a HMW inulin. For this reason, it was decided to test the growth of 13 different probiotic strains using this type of inulin nanoparticles as the only source of carbon. Fructose and FOS Orafti (inulin type

562    fructooligosaccharides) were used as a positive control whereas cultures without carbon

563    source were used as negative control.

564

565    Figure 7, shows the maximum optical density ($MOD_{600nm}$) reached after 48 hours of

566    culture. For fructose, similar growth was observed for all strains with $MOD_{600nm}$ between

567    1.53 and 1.68. Regarding FOS Orafti, values of $MOD_{600nm}$ between 1.43 and 1.63 were

568    registered. In contrast, no growth was observed when using HMW inulin as the only carbon

569    source, suggesting that this polymer has no prebiotic potential. The prebiotic character of

570    low molecular weight inulin (DP=36) has been reported before (Baston, Neagu Bonciu &

571    Bahrim, 2012). However, the high molecular weight of the inulin used in the present work

572    (DP=18500),  could be the limiting factor for the growth of probiotic strains.

573
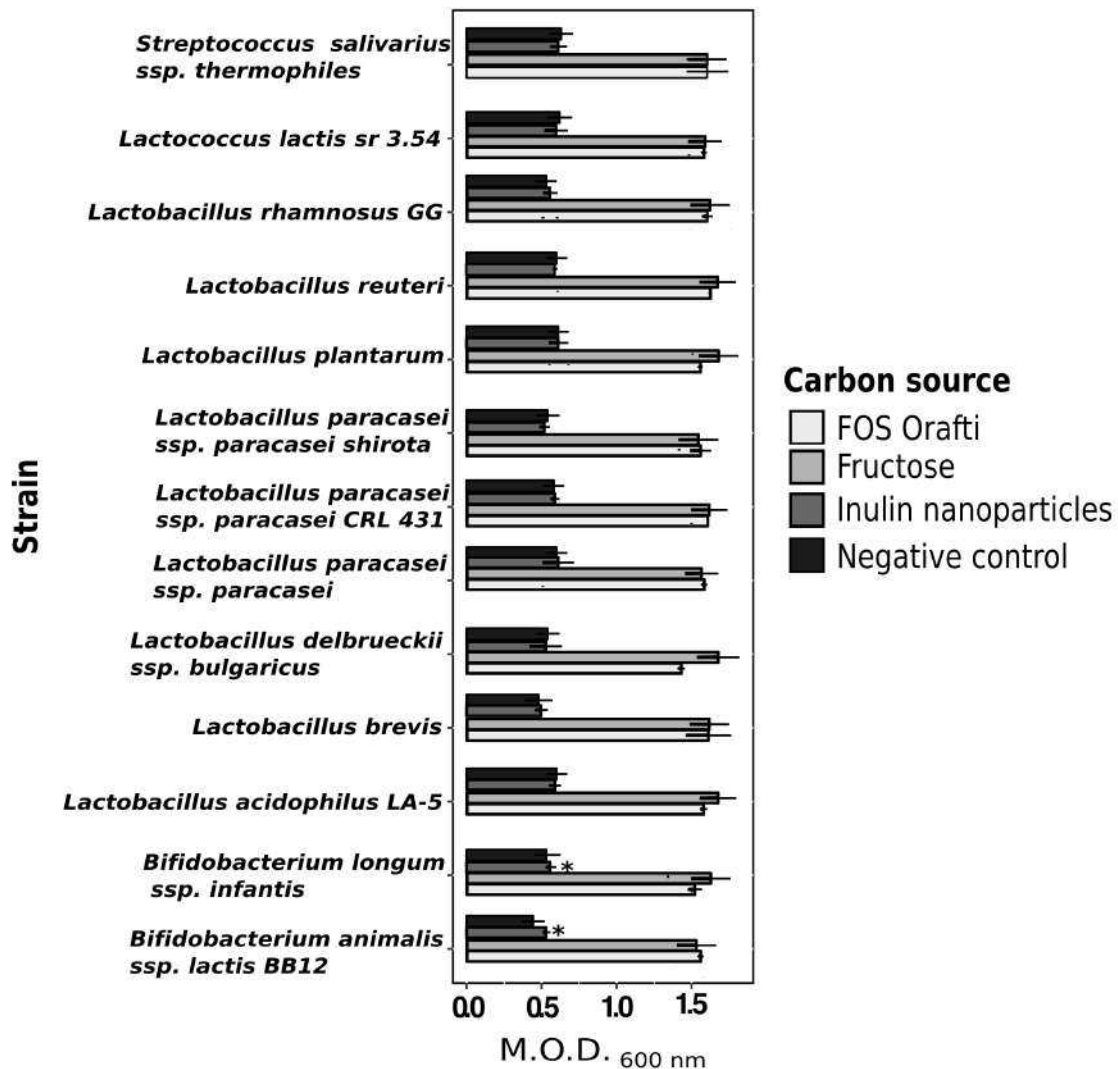
Figure 7. Maximum optical density (M.O.D. 600nm) of probiotic strains using fructose,

Orafti FOS, and HMW inulin, as the only carbon source. The M.O.D.600nm was measured

after 48 hours of incubation.

577

The results presented in this section demonstrate that the *Leuconostoc citreum* inulin

nanoparticles synthesized by the enzyme IslA do not show a prebiotic potential by the

strains studied, although a different outcome could be obtained *in vivo* as, the metabolism

581    of fructans in the intestinal tract is a cooperative process between different species

582    (syntrophism) (Rossi et al., 2005).

583

584    **4. Conclusion**

585    In the present study, a deep characterization of the physicochemical properties of HMW

586    inulin was performed; this particular fructan has a branching percentage of $10.03 \pm 1$ %,

587    higher than other reported for HMW inulins. HMW inulin is nanostructured in spherical

588    particles with a Z-average of the calculated diameter of $112 \pm 5$ nm and a polydispersity

589    index of $0.069 \pm 0.01$. The Zeta-potential of this nanoparticles was $-10 \pm 1.8$ mV, our

590    studies demonstrate that this slightly negative value is due to the presence of protein in the

591    nanoparticles. Although Zeta-potential value corresponds to particles with a tendency to

592    aggregate, stability assays demonstrated that inulin nanoparticles are stable at least for 15

593    days.

594

595    We also demonstrated that self-assembly of HMW inulin nanoparticles is carried out during

596    enzymatic synthesis of the polymer, observing the existence of a critical aggregation

597    concentration, which is influenced by the reaction temperature. The lower temperature of

598    the enzymatic reaction resulted in an increase of the nanoparticle size, reaching an average

599    hydrodynamic diameter of 131 nm. Under these conditions, other arrangements (fibers)

600    could be detected. Finally, we demonstrated that these nanoparticles are not toxic for

601    peripheral blood mononuclear cells, under concentrations as high as 200 μg/mL; besides,

602    no prebiotic potential was detected *in vitro* assays using individual probiotic strains.

603

604    In general, these results will allow us a better comprehension of the fructan nanoparticles

605    synthesis and factors that affect its synthesis, in order to manipulate the nanoparticle

606    production for example to regulate its size. The results of the biochemical and

607    physicochemical characterization suggest the HMW inulin nanoparticles could be used as a

608    novel drugs delivery system or other molecules of interest. Further work is in progress

609    regarding the encapsulation of biomolecules by these nanoparticles as well as its uptake by

610    eukaryotic cells; also immunomodulatory effect analysis of these HMW inulin

611    nanoparticles are still in progress.

612

619

620    **Author Contributions**

621    CO and MJS conceived the study and designed the experiments. MJS performed the

622    enzymatic experiments. MJS, WP, RL and FMG carried out analysis to the

623    physicochemical characterization of HMW inulin. MJS and GZP obtained the TEM

624    nanoparticles micrographies. RPM performed cytotoxicity test. MJS and MM carried out

625    the prebiotic potential analysis. CO, MJS, MA, MM, RPM, FMG and VBM analyzed data

626    and wrote the manuscript. All authors have given approval to the final version of the

627    manuscript.

628   **References**

629   Ahmed, H. B., Zahran, M. K., & Emam, H. E. (2016). Heatless synthesis of well

630       dispersible Au nanoparticles using pectin biopolymer. *International Journal of*

631       *Biological Macromolecules*, *91*, 208–219.

632       http://doi.org/10.1016/j.ijbiomac.2016.05.060

633   Amorij, J.-P., Meulenaar, J., Hinrichs, W. L. J., Stegmann, T., Huckriede, A., Coenen, F.,

634       & Frijlink, H. W. (2007). Rational design of an influenza subunit vaccine powder with

635       sugar glass technology: Preventing conformational changes of haemagglutinin during

636       freezing and freeze-drying. *Vaccine*, *25*(35), 6447–6457.

637       http://doi.org/10.1016/j.vaccine.2007.06.054

638   Baston, O., Neagu Bonciu, C., Bahrim, G. (2012). Preliminary study of lactic acid

639       production from inulin hydrolysates using *Lactobacillus acidophilus* LA-5. *Scientific*

640       *Bulletin. Series F. Biotechnologies*, *XVI*, 79–85. Retrieved from

641       http://www.biotechnologyjournal.usamv.ro/pdf/vol16/art14.pdf

642   Bhattacharjee, S. (2016). DLS and zeta potential – What they are and what they are not?

643       *Journal of Controlled Release*, *235*, 337–351.

644       http://doi.org/10.1016/j.jconrel.2016.06.017

645   Bradford, M. M. (1976). A rapid and sensitive method for the quantitation of microgram

646       quantities of protein utilizing the principle of protein-dye binding. *Analytical*

647       *Biochemistry*, *72*(1-2), 248–254. http://doi.org/10.1016/0003-2697(76)90527-3

648   Carneiro-Da-Cunha, M. G., Cerqueira, M. A., Souza, B. W. S., Teixeira, J. A., & Vicente,

649       A. A. (2011). Influence of concentration, ionic strength and pH on zeta potential and

650       mean hydrodynamic diameter of edible polysaccharide solutions envisaged for

651       multinanolayered films production. *Carbohydrate Polymers*, *85*(3), 522–528.

652      http://doi.org/10.1016/j.carbpol.2011.03.001

653      Chambert, R., & Gonzy-Treboul, G. (1976). Levansucrase of *Bacillus subtilis*: Kinetic and

654      Thermodynamic Aspects of Transfructosylation Processes. *European Journal of*

655      *Biochemistry*, *62*(1), 55–64. http://doi.org/10.1111/j.1432-1033.1976.tb10097.x

656      Cooper, P. D., Rajapaksha, K. H., Barclay, T. G., Ginic-Markovic, M., Gerson, A. R., &

657      Petrovsky, N. (2015). Inulin crystal initiation via a glucose-fructose cross-link of

658      adjacent polymer chains: Atomic force microscopy and static molecular modelling.

659      *Carbohydrate Polymers*, *117*(2), 964–972.

660      http://doi.org/10.1016/j.carbpol.2014.10.022

661      Cruz Herrera, L. (2012). *Caracterización de nanocompuestos de polietileno-co-octadeceno*

662      *con tio2, preparados mediante polimerización in-situ*. Universidad de Chile, Facultad

663      de Ciencias Físicas y Matemáticas.

664      Dan, A., Ghosh, S., & Moulik, S. P. (2009). Physicochemical studies on the biopolymer

665      inulin: A critical evaluation of its self-aggregation, aggregate-morphology, interaction

666      with water, and thermal stability. *Biopolymers*, *91*(9), 687–699.

667      http://doi.org/10.1002/bip.21199

668      Del Moral, S., Olvera, C., Rodriguez, M. E., & Munguia, A. L. (2008). Functional role of

669      the additional domains in inulosucrase (IslA) from *Leuconostoc citreum* CW28. *BMC*

670      *Biochemistry*, *9*(1), 1–10. http://doi.org/10.1186/1471-2091-9-6

671      Ebisu, S., Kato, K., Kotani, S., & Misaki, A. (1975). Structural differences in fructans

672      elaborated by S*treptococcus mutans* and *Strep. salivarius*. *J Biochem*, *78*(5), 879–887.

673      Retrieved from

674      http://www.ncbi.nlm.nih.gov/entrez/query.fcgi?cmd=Retrieve&db=PubMed&dopt=Ci

675      tation&list_uids=1213996

676   Fares, M. M., & Salem, M. S. (2015). Dissolution enhancement of curcumin via curcumin–

677        prebiotic inulin nanoparticles. *Drug Development and Industrial Pharmacy*, *Jan*

678        *30*(00), 1–8. http://doi.org/10.3109/03639045.2015.1004184

679   Handa, C., Goomer, S., & Siddhu, A. (2012). Physicochemical properties and sensory

680        evaluation of fructoligosaccharide enriched cookies. *Journal of Food Science and*

681        *Technology*, *49*(2), 192–199. http://doi.org/10.1007/s13197-011-0277-4

682   Hinrichs, W. L. J., Prinsen, M. G., & Frijlink, H. W. (2001). Inulin glasses for the

683        stabilization of therapeutic proteins. *International Journal of Pharmaceutics*, *215*(1-2),

684        163–174. http://doi.org/10.1016/S0378-5173(00)00677-3

685   Kim, S. J., Bae, P. K., & Chung, B. H. (2015). Self-assembled levan nanoparticles for

686        targeted breast cancer imaging. *Chemical Communications*, *51*(1), 107–110.

687        http://doi.org/10.1039/c4cc07679f

688   Kim, W. S., Lee, J. Y., Singh, B., Maharjan, S., Hong, L., Lee, S. M., Cho, C. S. (2018). A

689        new way of producing pediocin in *Pediococcus acidilactici* through intracellular

690        stimulation by internalized inulin nanoparticles. *Scientific Reports*, *8*(1), 1–14.

691        http://doi.org/10.1038/s41598-018-24227-z

692   Kumar, R., Manjunatha, S., Kathiravan, T., Vijayalakshmi, S., Nadanasabapathi, S., &

693        Raju, P. S. (2015). Rheological characteristics of inulin solution at low concentrations:

694        Effect of temperature and solid content. *Journal of Food Science and Technology*,

695        *52*(9), 5611–5620. http://doi.org/10.1007/s13197-014-1671-5

696   Li, R., Jiang, Z., Chen, F., Yang, H., & Guan, Y. (2004). Hydrogen bonded structure of

697        water and aqueous solutions of sodium halides: a Raman spectroscopic study. *Journal*

698        *of Molecular Structure*, *707*(1-3), 83–88.

699        http://doi.org/10.1016/j.molstruc.2004.07.016

700    Madrigal, L., & Sangronis, E. (2007). La inulina y derivados como ingredientes claves en

701        alimentos funcionales. *Archivos Latinoamericanos de Nutrición*, *57*(4), 387–396.

702        Retrieved from http://sportnutrition.sport.gov.mo/images/pt/img_osteo_g1.jpg

703    Makras, L., Van Acker, G., & De Vuyst, L. (2005). *Lactobacillus paracasei* subsp.

704        paracasei 8700:2 Degrades Inulin-Type Fructans Exhibiting Different Degrees of

705        Polymerization. *Applied and Environmental Microbiology*, *71*(11), 6531–6537.

706        http://doi.org/10.1128/AEM.71.11.6531-6537.2005

707    Miller, G. L. (1959). Use of Dinitrosalicylic Acid Reagent for Determination of Reducing

708        Sugar. *Analytical Chemistry*, *31*(3), 426–428. http://doi.org/10.1021/ac60147a030

709    Nakapong, S., Pichyangkura, R., Ito, K., Iizuka, M., & Pongsawasdi, P. (2013). High

710        expression level of levansucrase from *Bacillus licheniformis* RN-01 and synthesis of

711        levan nanoparticles. *International Journal of Biological Macromolecules*, *54*(1), 30–

712        36. http://doi.org/10.1016/j.ijbiomac.2012.11.017

713    Olivares-Illana,V. Wacher-Rodarte,C. Le Borgne,S. Lopez-Munguia,A. (2002).

714        Characterization of a cell-associated inulosucrase from a novel source: A *Leuconostoc*

715        *citreum* strain isolated from Pozol, a fermented corn beverage of Mayan origin.

716        *Journal of Industrial Microbiology & Biotechnology,* 28: 112-117.

717        https://doi.org/10.1038/sj/jim/700022

718    Ortiz-Soto, M. E., Olivares-Illana, V., & López-Munguía, A. (2004). Biochemical

719        properties of inulosucrase from *Leuconostoc citreum* CW28 used for inulin synthesis.

720        *Biocatalysis and Biotransformation*, *22*(4), 275–281.

721        http://doi.org/10.1080/10242420400014251

722    Porras-Domínguez, J. R., Ávila-Fernández, Á., Miranda-Molina, A., Rodríguez-Alegría, M.

723        E., & Munguía, A. L. (2015). *Bacillus subtilis* 168 levansucrase (SacB) activity affects

724      average levan molecular weight. *Carbohydrate Polymers*, *132*, 338–344.

725      http://doi.org/10.1016/j.carbpol.2015.06.056

726      Praznik W, Löppert R. & Helmut A. (2007). Analysis and molecular composition of

727      fructans from different plant sources. In *Recent Advances in Fructooligosaccharides*

728      (pp. 93–117).

729      Raga-Carbajal, E., Carrillo-Nava, E., Costas, M., Porras-Dominguez, J., López-Munguía,

730      A., & Olvera, C. (2016). Size product modulation by enzyme concentration reveals

731      two distinct levan elongation mechanisms in *Bacillus subtilis* levansucrase.

732      *Glycobiology*, *26*(4), 377–385. http://doi.org/10.1093/glycob/cwv112

733      Repetto, G., del Peso, A., & Zurita, J. L. (2008). Neutral red uptake assay for the estimation

734      of cell viability/cytotoxicity. *Nature Protocols*, *3*(7), 1125–1131.

735      http://doi.org/10.1038/nprot.2008.75

736      Roberfroid, M., & Slavin, J. (2000). Nondigestible Oligosaccharides. *Critical Reviews in*

737      *Food Science and Nutrition*, *40*(6), 461–480.

738      http://doi.org/10.1080/10408690091189239

739      Rolf, D., & Gray, G. R. (1984). Analysis of the linkage positions in d-fructofuranosyl

740      residues by the reductive-cleavage method. *Carbohydrate Research*, *131*(1), 17–28.

741      http://doi.org/10.1016/0008-6215(84)85399-9

742      Rossi, M., Corradini, C., Amaretti, A., Nicolini, M., Pompei, A., Zanoni, S., & Matteuzzi,

743      D. (2005). Fermentation of Fructooligosaccharides and Inulin by Bifidobacteria : a

744      Comparative Study of Pure and Fecal Cultures, *71*(10), 6150–6158.

745      http://doi.org/10.1128/AEM.71.10.6150

746      Santiago-Rodríguez, L., Lafontaine, M. M., Castro, C., Méndez-Vega, J., Latorre-Esteves,

747      M., Juan, E. J., … Rinaldi, C. (2013). Synthesis, Stability, Cellular Uptake, and Blood

748    Circulation Time of Carboxymethyl-Inulin Coated Magnetic Nanoparticles. *Journal of*

749    *Materials Chemistry. B, Materials for Biology and Medicine*, *1*(22), 2807–2817.

750    http://doi.org/10.1039/C3TB20256A

751  Sarkar, A., Ademuyiwa, V., Stubley, S., Esa, N. H., Goycoolea, F. M., Qin, X., … Olvera,

752    C. (2018). Pickering emulsions co-stabilized by composite protein/ polysaccharide

753    particle-particle interfaces: Impact on in vitro gastric stability. *Food Hydrocolloids*,

754    *84*, 282–291. http://doi.org/10.1016/j.foodhyd.2018.06.019

755  Sezer, A. D., Kazak, H., Öner, E. T., & Akbua, J. (2011). Levan-based nanocarrier system

756    for peptide and protein drug delivery: Optimization and influence of experimental

757    parameters on the nanoparticle characteristics. *Carbohydrate Polymers*, *84*(1), 358–

758    363. http://doi.org/10.1016/j.carbpol.2010.11.046

759  Sharma, N., Madan, P., & Lin, S. (2016). Effect of process and formulation variables on the

760    preparation of parenteral paclitaxel-loaded biodegradable polymeric nanoparticles: A

761    co-surfactant study. *Asian Journal of Pharmaceutical Sciences*, *11*(3), 404–416.

762    http://doi.org/10.1016/j.ajps.2015.09.004

763  Stephen, A., Phillips, G., & Williams, P. (Eds.). (2006). *Food Polysaccharides and Their*

764    *Applications*. CRC Press. http://doi.org/10.1201/9781420015164

765  Sundar, S., Kundu, J., & Kundu, S. C. (2010). Biopolymeric nanoparticles. *Science and*

766    *Technology of Advanced Materials*, *11*(1), 014104. http://doi.org/10.1088/1468-

767    6996/11/1/014104

768  Tabernero, A., González-Garcinuño, Á., Sánchez-Álvarez, J. M., Galán, M. A., & Martín

769    del Valle, E. M. (2017). Development of a nanoparticle system based on a fructose

770    polymer: Stability and drug release studies. *Carbohydrate Polymers*, *160*, 26–33.

771    http://doi.org/10.1016/j.carbpol.2016.12.025

772  Thanh, N. T. K., Maclean, N., & Mahiddine, S. (2014). Mechanisms of nucleation and

773      growth of nanoparticles in solution. *Chemical Reviews*, *114*(15), 7610–7630.

774      http://doi.org/10.1021/cr400544s

775  Vogt, L. M., Meyer, D., Pullens, G., Faas, M. M., Venema, K., Ramasamy, U., … de Vos,

776      P. (2014). Toll-Like Receptor 2 Activation by  2-&gt;1-Fructans Protects Barrier

777      Function of T84 Human Intestinal Epithelial Cells in a Chain Length-Dependent

778      Manner. *Journal of Nutrition*, *144*(7), 1002–1008.

779      http://doi.org/10.3945/jn.114.191643

780  Vogt, L., Ramasamy, U., Meyer, D., Pullens, G., Venema, K., Faas, M. M., … de Vos, P.

781      (2013). Immune Modulation by Different Types of β2→1-Fructans Is Toll-Like

782      Receptor Dependent. *PLoS ONE*, *8*(7), 1–12.

783      http://doi.org/10.1371/journal.pone.0068367

784  Wada, T., Sugatani, J., Terada, E., Ohguchi, M., & Miwa, M. (2005). Physicochemical

785      Characterization and Biological Effects of Inulin Enzymatically Synthesized from

786      Sucrose. *Journal of Agricultural and Food Chemistry*, *53*(4), 1246–1253.

787      http://doi.org/10.1021/jf048711u

788  Watzl, B., Girrbach, S., & Roller, M. (2005). Inulin, oligofructose and immunomodulation.

789      *British Journal of Nutrition*, *93*(S1), S49. http://doi.org/10.1079/BJN20041357

790  Wolff, D., Czapla, S., Heyer, A. G., Radosta, S., Mischnick, P., & Springer, J. (2000).

791      Globular shape of high molar mass inulin revealed by static light scattering and

792      viscometry, *41*, 0–7. https://doi.org/10.1016/S0032-3861(00)00168-3

793  Wongsagonsup, R., Shobsngob, S., Oonkhanond, B., & Varavinit, S. (2005). Zeta potential

794      and pasting properties of phosphorylated or crosslinked rice starches. *Starch/Staerke*,

795      *57*(1), 32–37. http://doi.org/10.1002/star.200400311

796    Zhang, L., Li, Y., Wang, C., Li, G., Zhao, Y., & Yang, Y. (2014). Synthesis of

797        methylprednisolone loaded ibuprofen modified inulin based nanoparticles and their

798        application for drug delivery. *Materials Science and Engineering C*, *42*, 111–115.

799        http://doi.org/10.1016/j.msec.2014.05.025

800